Hindawi
Advances in Civil Engineering
Volume 2019, Article ID 1684707, 10 pages
https://doi.org/10.1155/2019/1684707

Research Article

A New Unified Solution for Circular Tunnels Based on Generalized SMP Criterion considering the Strain Softening and Dilatancy

Qifeng Guo[1,2], **Jiliang Pan**[1,2], **Xinghui Wu**[1,2], **Xun Xi**[1,2] and **Meifeng Cai**[1,2]

[1]*School of Civil and Resource Engineering, University of Science and Technology Beijing, Beijing 100083, China*
[2]*Beijing Key Laboratory of Urban Underground Space Engineering, University of Science and Technology Beijing, Beijing 100083, China*

Correspondence should be addressed to Qifeng Guo; guoqifeng@ustb.edu.cn and Jiliang Pan; b20170008@xs.ustb.edu.cn

Received 28 December 2018; Revised 2 February 2019; Accepted 19 February 2019; Published 2 April 2019

Academic Editor: Hossein Moayedi

According to the strain-softening characteristics of rock mass, an ideal elastic strain-softening model is developed, and the surrounding rock of tunnels is subdivided into the plastic broken zone, plastic strain-softening zone, and elastic zone. Based on the generalized spatially mobilized plane criterion, an elastic-plastic analytical solution of a circular tunnel is derived. The effects of intermediate principal stress, strain softening, and dilatancy are considered in the unified solution. The stress, displacement, and plastic zone radius of surrounding rock based on the SMP criterion are compared with those based on the Mohr–Coulomb criterion. Furthermore, the effects of parameters such as the softening modulus, dilatancy angle, and internal friction angle on the deformation and stress of tunnels are discussed. It has been found that the larger the dilatancy angle is, the larger the plastic zone displacement and the radius of the broken zone are. The larger the internal friction angle, the smaller the sizes of the plastic zone, the strain-softening zone, and the broken zone are. The deformation of surrounding rock in the broken zone is more sensitive to the internal friction angle than that in the strain-softening zone. The unified solution based on the SMP criterion provides a well understanding for the elastic-plastic state of tunnels, which can be the guidance for tunnel excavations and support designs.

1. Introduction

Rock tunnels are common underground constructions for mining engineering, traffic engineering, diversion engineering, and nuclear waste disposal engineering. The stress around tunnels redistributes due to the excavation disturbance. The concentrated stress usually exceeds ultimate strengths of the surrounding rock, which make the rock properties transform from elastic state to plastic state. Based on the ideal elastic-plastic model, Fenner and Kastner analyzed the elastic and plastic zones of tunnels and derived Fenner formula and Kastner formula [1]. Terzaghi and Peck first proposed that geotechnical materials have strain-softening characteristics [2]. Then considerable researches have indicated that, after the stress of geomaterials exceeds the compressive strength, the stress of the geomaterials will gradually decrease to the residual strength with the strain increasing [3–8]. Therefore, the strain-softening characteristics of the surrounding rock must be considered in the elastic-plastic analysis of tunnels.

Determination of the plastic zone of a tunnel is an important foundation for the stability analysis and support design of the tunnel. Analytical solutions of circular tunnels can provide a fast and direct understanding for tunnels elastic-plastic state, which is an important part in geotechnical analyses [9, 10]. Traditional elastic-plastic analytical solutions of tunnels are generally based on the Mohr–Coulomb criterion or the Hoek–Brown criterion, in which the effect of the intermediate principal stress is not considered. Although the Drucker–Prager criterion includes the intermediate principal stress, it does not consider the strength differential effect of geomaterials in the deviator stress plane [11–17].

Previous studies have shown that the geomaterials have a phenomenon of volume expansion during the postpeak deformation process, which is called "dilatancy." The dilatancy is closely related to the plastic shear strain and the strength parameters of rock mass [18–20]. Therefore, in the elastic-plastic analysis of tunnels, the effects of intermediate principal stress, strain softening, and dilatancy should be considered comprehensively.

In this paper, an ideal elastic strain-softening model is first developed and the surrounding rock of circular tunnels is subdivided into the plastic broken zone, plastic strain-softening zone, and elastic zone. Based on the generalized SMP (i.e., spatially mobilized plane) criterion, a rational analytical solution of the circular tunnel is derived in consideration of the effects of the intermediate principal stress, strain softening, and dilatancy. The stress distribution, displacement distribution, and plastic zone radius of surrounding rock calculated by the solution based on the SMP criterion are compared with those based on the Mohr–Coulomb criterion. Finally, parametric studies of softening modulus, dilatancy angle, and internal friction angle are carried out.

2. Generalized SMP Criterion

The theory of spatially mobilized plane for noncohesive soils is proposed by Matsuoka and Nakai, referred to as the SMP failure criterion [21]. The SMP criterion has a good agreement with the Mohr–Coulomb criterion. Moreover, it overcomes the singularity of the Mohr–Coulomb criterion in the deviator stress plane and the equivalence of strengths of the Drucker–Prager criterion. In addition, the SMP criterion also reflects the effect of intermediate principal stress. The SMP criterion is expressed as [22]

$$\frac{\tau_{\mathrm{SMP}}}{\sigma_{\mathrm{SMP}}} = \frac{2}{3}\sqrt{\frac{(\sigma_1-\sigma_2)^2}{4\sigma_1\sigma_2} + \frac{(\sigma_2-\sigma_3)^2}{4\sigma_2\sigma_3} + \frac{(\sigma_3-\sigma_1)^2}{4\sigma_3\sigma_1}} = \text{const}, \tag{1}$$

where τ_{SMP} and σ_{SMP} are the shear and normal stresses on the SMP, respectively, and σ_1, σ_2, and σ_3 are the large, medium, and small principal stresses of the noncohesive soil, respectively.

Figure 1 shows the mutual relationship between the Mohr–Coulomb criterion and SMP criterion in the π plane. It can be seen that, the limiting trajectory of the SMP criterion in the π plane is a smoothly convex curve circumscribing the irregularly hexagon of the Mohr–Coulomb criterion.

Matsuoka et al. revised the SMP criterion by introducing a bond stress σ_0 and further extended the SMP criterion to cohesive soil [22, 23]. According to the SMP criterion, when the noncohesive soil is destroyed in the plane strain state, the common tangent of the Mohr circle of limit stress on the τ-σ space just passes through the coordinate origin. When the general clay soil is destroyed in the plane strain state, the common tangent of the Mohr circle of limit stress on the τ-σ space just passes the bond stress point σ_0 [24, 25]. The limit stress state of generalized SMP criterion in the plane strain condition is shown in Figure 2.

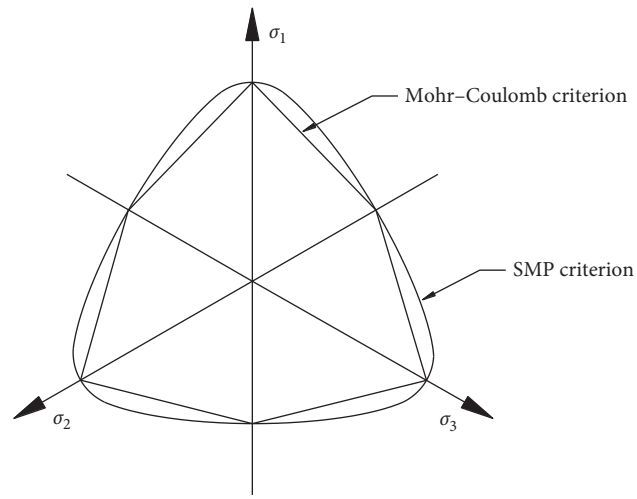

Figure 1: Mutual relationship between the Mohr–Coulomb criterion and SMP criterion in the π plane.

For the materials containing cohesion c and internal friction angle φ, the failure criterion in the plane strain condition can be written as

$$\tau = c + \sigma \tan\varphi. \tag{2}$$

The bond stress σ_0 can be obtained as

$$\sigma_0 = c\cot\varphi. \tag{3}$$

The generalized SMP criterion expressed by stress invariants is as follows:

$$\frac{\widetilde{I}_1\widetilde{I}_2}{\widetilde{I}_3} = 8\tan^2\varphi + 9 = K_{\mathrm{SMP}}, \tag{4}$$

where φ is the internal friction angle obtained by the triaxial test; K_{SMP} is the material constant of the SMP criterion; and $\widetilde{I}_1$, $\widetilde{I}_2$, and $\widetilde{I}_3$ are the generalized first, second, and third effective stress invariants, respectively. The effective stress invariants are given as follows by using the principal stress σ_i and the bond stress σ_0:

$$\begin{aligned}
\widetilde{I}_1 &= (\sigma_1+\sigma_0)+(\sigma_2+\sigma_0)+(\sigma_3+\sigma_0),\\
\widetilde{I}_2 &= (\sigma_1+\sigma_0)(\sigma_2+\sigma_0)+(\sigma_2+\sigma_0)(\sigma_3+\sigma_0)\\
&\quad +(\sigma_3+\sigma_0)(\sigma_1+\sigma_0),\\
\widetilde{I}_3 &= (\sigma_1+\sigma_0)(\sigma_2+\sigma_0)(\sigma_3+\sigma_0).
\end{aligned} \tag{5}$$

According to the associated flow rule and the generalized SMP criterion, the relationship among σ_1, σ_2, and σ_3 in the plane strain condition can be expressed as follows:

$$\sigma_2 + \sigma_0 = \sqrt{(\sigma_1+\sigma_0)(\sigma_3+\sigma_0)}. \tag{6}$$

Substituting (6) in (4), the expression of the generalized SMP criterion in the plane strain condition is as follows:

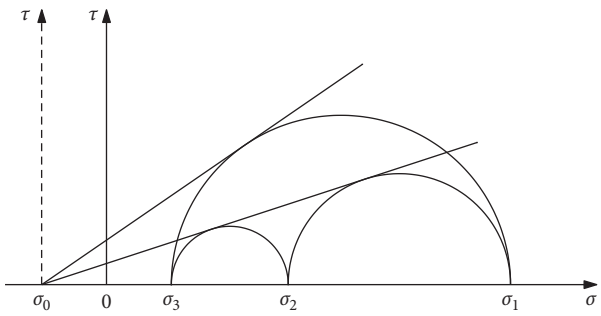

Figure 2: Limit stress state of generalized SMP criterion in the plane strain condition.

$$\frac{\sigma_1+\sigma_0}{\sigma_3+\sigma_0}=\frac{1}{4}\left[\sqrt{K_{\mathrm{SMP}}}-1+\sqrt{\left(\sqrt{K_{\mathrm{SMP}}}-1\right)^2-4}\right]^2. \quad (7)$$

The tangential stress σ_θ, radial stress σ_r, and axial stress σ_z of the tunnel are orthogonal to each other. When the lateral pressure coefficient $\lambda = 1$, the stresses σ_θ, σ_r, and σ_z can be regarded as three principal stresses. It can be regarded that the three principal stresses in surrounding rock of circular tunnels are $\sigma_1 = \sigma_\theta$, $\sigma_3 = \sigma_r$, and $\sigma_2 = \sigma_z$. Formula (7) can be written as

$$f = \sigma_\theta - M\sigma_r - N = 0, \quad (8)$$

where

$$M=\frac{1}{4}\left[\sqrt{8\tan^2\varphi+9}-1+\sqrt{\left(\sqrt{8\tan^2\varphi+9}-1\right)^2-4}\right]^2,$$

$$N=(M-1)c\cot\varphi. \quad (9)$$

3. Description of the Elastic-Plastic Model

3.1. Strain-Softening Model. Considerable laboratory tests and field observations have indicated that, after the stress of the rock exceeds its compressive strength, the stress will gradually decrease to the residual strength [3–8]. According to the strain-softening characteristics of the surrounding rock, the strain-softening model is established as shown in Figure 3. The rock mass in the elastic zone is far away from the tunnel. The rock mass in the broken zone is near the surface of the tunnel with residual strength. And the plastic strain-softening zone is the area between the elastic zone and the broken zone.

3.2. Calculation Model of Circular Tunnels. In order to carry out the elastic-plastic analysis of surrounding rock, the following assumptions are made:

(1) The cross section of the tunnel is in circular shape and the length is infinite. So it can be simplified as a plane strain problem.

(2) Rock mass is a continuous, homogeneous, and isotropic elastic-plastic material.

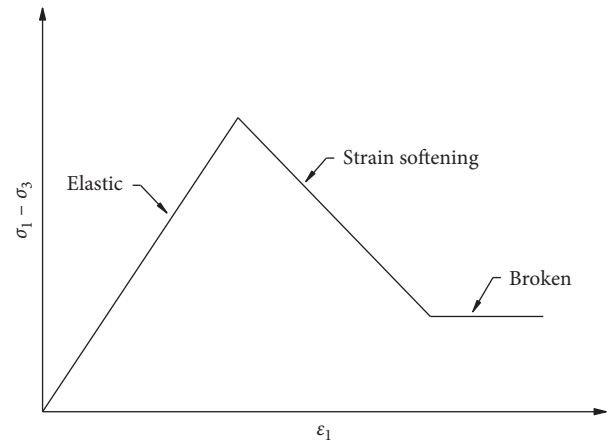

Figure 3: Elastic strain-softening model of the rock.

(3) Ignoring the effects of the surrounding rock weight on the yield, the original rock stress can be simplified as a uniform stress distribution. The tunnel is under the conditions of uniform stress p_0 and support resistance p_i.

(4) The plastic zone induced by the excavation is subdivided into two parts: the plastic strain-softening zone and the plastic broken zone. The radius of the broken zone and the strain-softening zone are R_b and R_s, respectively.

The radius of the circular tunnel is r_0. Based on the above assumptions, the mechanical model of the tunnel is shown in Figure 4.

3.3. Softening Model of the Strength Parameter. The strain-softening characteristics of the rock mass can be reflected by strength parameters such as cohesion c or internal friction angle φ. The internal friction angle φ is not sensitive to the strain-softening characteristics of the rock mass, while the cohesion c is obviously affected by the strain-softening characteristics of rock mass [5, 26, 27]. Therefore, the cohesion c is used to represent the strain-softening characteristics of rock mass. The softening process of cohesion c is mainly related to the shear strain ε_θ^s of the strain-softening zone. The softening process is assumed as linear. The degree of softening is represented by the angle α and the corresponding softening modulus $H_c = \tan\alpha$. Therefore, the softening model of the strength parameter is shown as Figure 5.

c_0 and c^* in Figure 5 is the initial cohesion and residual cohesion, respectively. The shear strain at the interface between the elastic zone and the strain-softening zone is ε_θ^{e-s}, and the shear strain at the interface of the strain-softening zone and the broken zone is ε_θ^{s-b}. The cohesion c of a point in the surrounding rock of the circular tunnel can be expressed as follows:

$$c=\begin{cases} c_0, & r\ge R_s,\\ c_0-H_c\left(\varepsilon_\theta^s-\varepsilon_\theta^{e-s}\right), & R_b\le r\le R_s,\\ c^*, & r_0\le r\le R_b, \end{cases} \quad (10)$$

where $H_c = \tan\alpha = (c_0 - c^*)/(\varepsilon_\theta^{s-b} - \varepsilon_\theta^{e-s})$.

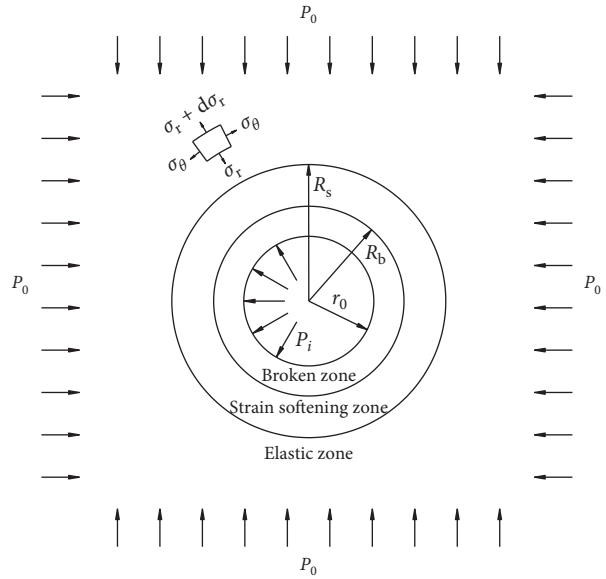

Figure 4: Mechanical model of the circular tunnel.

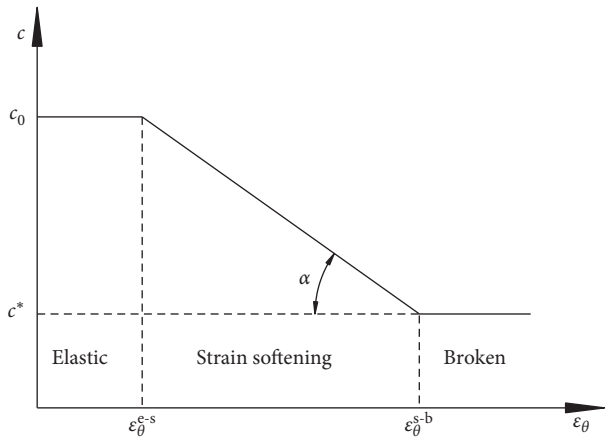

Figure 5: Softening model of the strength parameter.

3.4. Dilatancy Model. With the surrounding rock deformation and crushing, the volume of rock will expand. According to the plastic potential theory, the plastic strain increment can be expressed as follows [28]:

$$d\varepsilon_{ij}^{p} = d\lambda \frac{\partial g}{\partial \sigma_{ij}}, \tag{11}$$

where $d\varepsilon_{ij}^{p}$ is the plastic strain increment; $d\lambda$ is the plastic factor increment; g is the plastic potential function; and σ_{ij} is the stress tensor.

In order to reflect the dilatancy characteristics of the surrounding rock, it is assumed that the plastic potential function g has the same form as the yield function f. And the internal friction angle φ in the yield function is replaced by the dilatancy angle ψ. Thus, the plastic potential function g can be expressed as follows:

$$g = \sigma_\theta - M^* \sigma_r - N^*, \tag{12}$$

where

$$M^* = \frac{1}{4}\left[\sqrt{8\tan^2\psi + 9} - 1 + \sqrt{\left(\sqrt{8\tan^2\psi + 9} - 1\right)^2 - 4}\right]^2,$$
$$N^* = \left(M^* - 1\right)c\cot\psi. \tag{13}$$

Substituting (12) into (11), the plastic strain increment can be obtained as

$$d\varepsilon_\theta^{p} = d\lambda \frac{\partial g}{\partial \sigma_\theta} = d\lambda,$$
$$d\varepsilon_r^{p} = d\lambda \frac{\partial g}{\partial \sigma_r} = -M^* d\lambda. \tag{14}$$

Based on the linear nonassociative flow rule, the relationship of plastic strain increment can be expressed as [29]

$$\Delta\varepsilon_r^{p} + \chi\Delta\varepsilon_\theta^{p} = 0. \tag{15}$$

The expression of dilatancy coefficient in the strain-softening zone and broken zone is obtained by simultaneous (14) and (15):

$$\chi_1 = \frac{\Delta\varepsilon_r^{p}}{\Delta\varepsilon_\theta^{p}} = M^{s*},$$
$$\chi_2 = \frac{\Delta\varepsilon_r^{p}}{\Delta\varepsilon_\theta^{p}} = M^{b*}, \tag{16}$$

where M^{s*} and M^{b*} are the parameters for replacing the internal friction angle φ with the dilatancy angle ψ^s in the strain-softening zone and the dilatancy angle ψ^b in the broken zone, respectively. When $\psi = \varphi$, the uncorrelated flow law is transformed into the associated flow rule. When $\psi = 0^\circ$, the dilatancy characteristics of the rock are not considered.

4. Unified Solution of the Surrounding Rock of Circular Tunnels

4.1. Basic Equation. Based on the elastic-plastic theory, the equilibrium equation of the infinitesimal body around the tunnel can be expressed as

$$\frac{d\sigma_r}{dr} + \frac{\sigma_r - \sigma_\theta}{r} = 0. \tag{17}$$

In addition, strain-displacement relations of the surrounding rock are given as

$$\varepsilon_r = \frac{du}{dr},$$
$$\varepsilon_\theta = \frac{u}{r}. \tag{18}$$

After the strain components and displacement are obtained, the stress-strain relation involved in the plane strain problem can be expressed as

$$\varepsilon_{\mathrm{r}} = \frac{1-\nu^2}{E}\left(\sigma_{\mathrm{r}} - \frac{\nu}{1-\nu}\sigma_\theta\right),$$
$$\varepsilon_\theta = \frac{1-\nu^2}{E}\left(\sigma_\theta - \frac{\nu}{1-\nu}\sigma_{\mathrm{r}}\right). \tag{19}$$

4.2. Stress and Displacement in the Elastic Zone. Boundary conditions of the elastic zone can be given by

$$\sigma_{\mathrm{r}}^{\mathrm{e}} = \sigma_0, \quad \text{at } r = \infty,$$
$$\sigma_{\mathrm{r}}^{\mathrm{e}} = \sigma_{\mathrm{r}}^{\mathrm{e-s}}, \quad \text{at } r = R_{\mathrm{s}}, \tag{20}$$

where $\sigma_{\mathrm{r}}^{\mathrm{e-s}}$ is the radial stress at the interface between the elastic zone and the plastic strain-softening zone.

At the elastic-plastic interface, both failure criterion (8) and the following relationship are satisfied:

$$\sigma_{\mathrm{r}}^{\mathrm{e}} + \sigma_\theta^{\mathrm{e}} = 2\sigma_0. \tag{21}$$

The radial stress at the elastic-plastic interface can be obtained as

$$\sigma_{\mathrm{r}}^{\mathrm{e-p}} = \frac{2\sigma_0 - N^{\mathrm{e}}}{1 + M^{\mathrm{e}}}, \tag{22}$$

where M^{e} and N^{e} are the parameters M and N in the elastic zone, respectively.

According to the elastic-plastic theory, the elastic solutions of stress components can be expressed as

$$\sigma_{\mathrm{r}}^{\mathrm{e}} = \sigma_0 - \left(\sigma_0 - \sigma_{\mathrm{r}}^{\mathrm{e-p}}\right)\left(\frac{R_{\mathrm{s}}}{r}\right)^2,$$
$$\sigma_\theta^{\mathrm{e}} = \sigma_0 + \left(\sigma_0 - \sigma_{\mathrm{r}}^{\mathrm{e-p}}\right)\left(\frac{R_{\mathrm{s}}}{r}\right)^2. \tag{23}$$

According to the small deformation theory, the elastic solutions of strain components can be expressed as

$$\varepsilon_{\mathrm{r}}^{\mathrm{e}} = -\frac{1+\nu}{E}\left(\sigma_0 - \sigma_{\mathrm{r}}^{\mathrm{e-p}}\right)\frac{R_{\mathrm{s}}^2}{r^2},$$
$$\varepsilon_\theta^{\mathrm{e}} = \frac{1+\nu}{E}\left(\sigma_0 - \sigma_{\mathrm{r}}^{\mathrm{e-p}}\right)\frac{R_{\mathrm{s}}^2}{r^2}. \tag{24}$$

Substituting equation (24) into equation (18), the radial displacement component u^{e} of the tunnel surrounding rock in the elastic zone can be expressed as follows:

$$u^{\mathrm{e}} = \frac{1}{2G}\left(\sigma_0 - \sigma_{\mathrm{r}}^{\mathrm{e-p}}\right)\frac{R_{\mathrm{s}}^2}{r}, \tag{25}$$

where $G = E/2(1+\nu)$.

4.3. Stress and Displacement in the Plastic Strain-Softening Zone. According to the elastic-plastic theory, the strain in the strain-softening zone is composed of elastic strain and plastic strain which can be written as

$$\varepsilon_{\mathrm{r}}^{\mathrm{s}} = \varepsilon_{\mathrm{r}}^{\mathrm{se}} + \varepsilon_{\mathrm{r}}^{\mathrm{sp}},$$
$$\varepsilon_\theta^{\mathrm{s}} = \varepsilon_\theta^{\mathrm{se}} + \varepsilon_\theta^{\mathrm{sp}}, \tag{26}$$

where se and sp represents the elastic part and plastic part in the strain-softening zone, respectively.

By letting

$$f(r) = \varepsilon_r^{\mathrm{s}} + \chi\varepsilon_\theta^{\mathrm{s}}, \tag{27}$$

and combining equations (15) and (26), the equation for $f(r)$ can be obtained as follows:

$$f(r) = \left(\varepsilon_{\mathrm{r}}^{\mathrm{se}} + \chi\varepsilon_\theta^{\mathrm{se}}\right) + \left(\varepsilon_{\mathrm{r}}^{\mathrm{sp}} + \chi\varepsilon_\theta^{\mathrm{sp}}\right) = \varepsilon_{\mathrm{r}}^{\mathrm{se}} + \chi\varepsilon_\theta^{\mathrm{se}}. \tag{28}$$

Ignoring the effect of stress redistribution on the elastic strain in the strain-softening zone and regarding the elastic strain of the strain-softening zone as the same with the strain of the elastic zone at the elastic-plastic interface, the elastic strain in the strain-softening zone can be expressed as

$$\varepsilon_{\mathrm{r}}^{\mathrm{se}} = \varepsilon_{\mathrm{r}}^{\mathrm{e}}\big|_{r=R_{\mathrm{s}}},$$
$$\varepsilon_\theta^{\mathrm{se}} = \varepsilon_\theta^{\mathrm{e}}\big|_{r=R_{\mathrm{s}}}. \tag{29}$$

Substituting equations (28) and (29) into equation (18), $f(r)$ can be obtained as

$$f(r) = \varepsilon_{\mathrm{r}}^{\mathrm{e}}\big|_{r=R_{\mathrm{s}}} + \chi\varepsilon_\theta^{\mathrm{e}}\big|_{r=R_{\mathrm{s}}} = \frac{du^{\mathrm{s}}}{dr} + \chi\frac{u^{\mathrm{s}}}{r}. \tag{30}$$

In combination with the boundary condition at the elastic-plastic interface:

$$u^{\mathrm{s}} = u^{\mathrm{e-p}} = \frac{\left(\sigma_0 - \sigma_{\mathrm{r}}^{\mathrm{e-p}}\right)R_{\mathrm{s}}}{2G}, \text{ at } r = R_{\mathrm{s}}. \tag{31}$$

The displacement expression of the strain-softening zone is calculated as

$$u^{\mathrm{s}} = r\frac{\left(\sigma_0 - \sigma_{\mathrm{r}}^{\mathrm{e-p}}\right)}{2G(1+\chi)}\left[\chi - 1 + 2\left(\frac{R_{\mathrm{s}}}{r}\right)^{1+\chi}\right]. \tag{32}$$

Combining equations (18) and (32), the strain in the strain-softening zone can be obtained:

$$\varepsilon_{\mathrm{r}}^{\mathrm{s}} = \frac{(\chi-1)\left(\sigma_0 - \sigma_{\mathrm{r}}^{\mathrm{e-p}}\right)}{2G(1+\chi)} - \frac{\chi\left(\sigma_0 - \sigma_{\mathrm{r}}^{\mathrm{e-p}}\right)}{G(1+\chi)}\left(\frac{R_{\mathrm{s}}}{r}\right)^{1+\chi},$$
$$\varepsilon_\theta^{\mathrm{s}} = \frac{(\chi-1)\left(\sigma_0 - \sigma_{\mathrm{r}}^{\mathrm{e-p}}\right)}{2G(1+\chi)} + \frac{\sigma_0 - \sigma_{\mathrm{r}}^{\mathrm{e-p}}}{G(1+\chi)}\left(\frac{R_{\mathrm{s}}}{r}\right)^{1+\chi}. \tag{33}$$

Furthermore, the following equation can be obtained:

$$\varepsilon_\theta^{\mathrm{s}} - \varepsilon_\theta^{\mathrm{e-s}} = \frac{\sigma_0 - \sigma_{\mathrm{r}}^{\mathrm{e-p}}}{G(1+\chi)}\left[\left(\frac{R_{\mathrm{s}}}{r}\right)^{1+\chi} - 1\right],$$
$$\varepsilon_\theta^{\mathrm{s-b}} - \varepsilon_\theta^{\mathrm{e-s}} = \frac{\sigma_0 - \sigma_{\mathrm{r}}^{\mathrm{e-p}}}{G(1+\chi)}\left[\left(\frac{R_{\mathrm{s}}}{R_{\mathrm{b}}}\right)^{1+\chi} - 1\right]. \tag{34}$$

According to equation (10), the expression of the cohesive force in the strain-softening zone can be obtained:

$$c^{\mathrm{s}} = c_0 - H_{\mathrm{c}}\frac{\sigma_0 - \sigma_{\mathrm{r}}^{\mathrm{e-p}}}{G(1+\chi)}\left[\left(\frac{R_{\mathrm{s}}}{r}\right)^{1+\chi} - 1\right]. \tag{35}$$

Substitute equation (35) into the yield equation (8), replace the initial cohesion c_0, combined with (17) and the boundary conditions at the elastic-plastic interface,

$$\sigma_r^e = \sigma_r^{e-p}, \quad \text{at } r = R_s. \tag{36}$$

The radial and stress in the strain-softening zone can be obtained:

$$\begin{aligned}\sigma_r^s &= \left(\sigma_r^{e-p} - \frac{N^s}{1-M^s}\right)\left(\frac{R_s}{r}\right)^{1-M^s} + \frac{N^s}{1-M^s},\\ \sigma_\theta^s &= M^s\left(\sigma_r^{e-p} - \frac{N^s}{1-M^s}\right)\left(\frac{R_s}{r}\right)^{1-M^s} + \frac{N^s}{1-M^s},\end{aligned} \tag{37}$$

where M^s and N^s are the parameters M and N in the strain-softening zone, respectively.

4.4. Analysis of the Plastic Broken Zone. Substituting equation (8) into equation (17), The radial and stress in the broken zone can be solved by considering the boundary condition $\sigma_r^b = p_i$ at $r = r_0$:

$$\begin{aligned}\sigma_r^b &= \left(p_i - \frac{N^b}{1-M^b}\right)\left(\frac{r_0}{r}\right)^{1-M^b} + \frac{N^b}{1-M^b},\\ \sigma_\theta^b &= M^b\left(p_i - \frac{N^b}{1-M^b}\right)\left(\frac{r_0}{r}\right)^{1-M^b} + \frac{N^b}{1-M^b},\end{aligned} \tag{38}$$

where M^b and N^b are the parameters M and N in the broken zone, respectively.

The strain in the broken zone is also composed of elastic strain and plastic strain, and it satisfies $\varepsilon_r^{be} = \varepsilon_r^s$ and $\varepsilon_\theta^{be} = \varepsilon_\theta^s$ at $r = R_b$:

$$\begin{aligned}\varepsilon_r^b &= \varepsilon_r^{s-b} + \varepsilon_r^{bp},\\ \varepsilon_\theta^b &= \varepsilon_\theta^{s-b} + \varepsilon_\theta^{bp}.\end{aligned} \tag{39}$$

By equation (33), the strain in the broken zone can be obtained as

$$\begin{aligned}\varepsilon_r^{s-b} &= \frac{(\chi-1)(\sigma_0-\sigma_r^{e-p})}{2G(1+\chi)} - \frac{\chi(\sigma_0-\sigma_r^{e-p})}{G(1+\chi)}\left(\frac{R_s}{R_b}\right)^{1+\chi},\\ \varepsilon_\theta^{s-b} &= \frac{(\chi-1)(\sigma_0-\sigma_r^{e-p})}{2G(1+\chi)} + \frac{\sigma_0-\sigma_r^{e-p}}{G(1+\chi)}\left(\frac{R_s}{R_b}\right)^{1+\chi}.\end{aligned} \tag{40}$$

According to the same radial displacement at the interface between the strain-softening zone and the broken zone, the following equation can be obtained:

$$u^b\big|_{r=R_b} = u^{s-b} = R_b\frac{(\sigma_0-\sigma_r^{e-p})}{2G(1+\chi)}\left[\chi - 1 + 2\left(\frac{R_s}{R_b}\right)^{1+\chi}\right]. \tag{41}$$

We can get the expression of the displacement in the broken zone:

$$\begin{aligned}u^b = r\frac{\sigma_0-\sigma_r^{e-p}}{G}&\left\{\frac{1}{1+\chi_1}\left(\frac{R_s}{R_b}\right)^{1+\chi_1} + \frac{1}{1+\chi_2}\left(\frac{R_s}{R_b}\right)^{1+\chi_1}\right.\\ &\left.\cdot\left[\left(\frac{R_b}{r}\right)^{1+\chi_2} - 1\right] - \frac{1-\chi_1}{2(1+\chi_1)}\right\}.\end{aligned} \tag{42}$$

The displacement at the wall of the circular tunnel can be obtained by substituting $r = r_0$ into equation (42).

4.5. Radius of the Strain-Softening Zone. The radial stress at the interface between the strain-softening zone and the broken zone is continuous. And the cohesion c_0 is reduced to the residual value at the interface. By equations (36) and (37), the expression of the ratio of the strain-softening zone radius R_s to the circular tunnel radius r_0 can be obtained as

$$\frac{R_s}{r_0} = \sqrt[1-M^b]{\frac{(1-M^b)p_i - N^b}{(1-M^b)\sigma_r^{e-p} - N^b}}. \tag{43}$$

4.6. Radius of the Plastic Broken Zone. According to equation (10), the residual cohesion c^* at the interface between the strain-softening zone and the broken zone can be expressed as

$$c^* = c_0 - H_c\frac{\sigma_0-\sigma_r^{e-p}}{G(1+\chi)}\left[\left(\frac{R_s}{R_b}\right)^{1+\chi_1} - 1\right]. \tag{44}$$

The ratio of the strain-softening zone radius R_s to the broken zone radius R_b can be obtained as

$$\frac{R_s}{R_b} = \left[1 + \frac{G(1+\chi)(c_0-c^*)}{(\sigma_0-\sigma_r^{e-p})H_c}\right]^{1/(1+\chi_1)}. \tag{45}$$

5. Worked Examples and Parametric Studies

Taking a circular tunnel with the radius $r_0 = 3$ m as an example, the geometrical and mechanical parameters are shown in Table 1. The developed elastic-plastic model is used to analyze the stress and displacement of the tunnel.

The Mohr–Coulomb criterion is one of the most commonly used strength criteria in geotechnical engineering. The stress distribution of surrounding rock for the SMP criterion and the Mohr–Coulomb criterion are shown as Figures 6 and 7. It can be seen that the radial tangential stress distributions based on the SMP criterion and the Mohr–Coulomb criterion are different. The radial stress increases with radius increasing, but the growth rate gradually slows down. With the radius increasing, the tangential stress increases in the plastic zone, reaches a maximum value at the elastic-plastic interface, and then gradually decreases. Both radial and tangential stress will eventually be close to the initial rock stress. In addition, it can be seen that the radius of the plastic zone calculated by the SMP criterion is smaller than that of the Mohr–Coulomb criterion.

Figure 8 shows the displacement distribution and the radius of the plastic zone based on the SMP criterion and the Mohr–Coulomb criterion. The dotted vertical line indicates the radius of the broken zone, and the solid vertical line indicates the radius of the strain-softening zone. It can be seen that the displacement of the surrounding rock decreases with the radius increasing. The displacement of the surrounding rock based on the SMP criterion is generally smaller than that based on the Mohr–Coulomb criterion,

Table 1: Geometrical and mechanical parameters.

Symbol	Description	Value
E (GPa)	Elastic modulus	1.28
N	Poisson's ratio	0.22
c_0 (MPa)	Initial cohesion	3.8
c^* (MPa)	Residual cohesion	1.8
φ_0 (°)	Initial internal friction angle	26
φ^* (°)	Residual internal friction angle	14
ψ^s (°)	Dilatancy angle of the strain-softening zone	13
ψ^b (°)	Dilatancy angle of the broken zone	7
σ_0 (MPa)	In situ stress	20.0
p_i (MPa)	Support force	1
H_c (MPa)	Strain-softening modulus	200

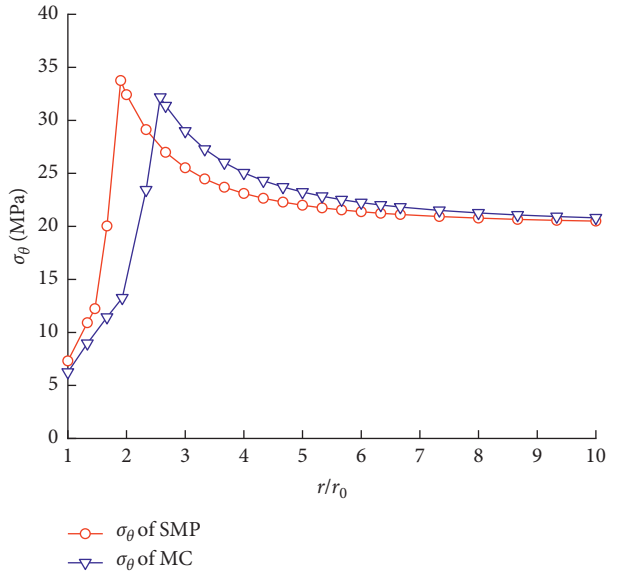

Figure 6: Surrounding rock radial stress distribution of the Mohr–Coulomb and SMP criteria.

and the difference between them decreases with the increase of the radius. The displacement will eventually tend to be 0 m as the radius increases. At the tunnel surface, the displacement based on the SMP criterion is 16.67 mm. The maximum displacement based on the Mohr–Coulomb criterion is 28.85 mm, which is 1.73 times larger than that based on the SMP criterion. The radius of the broken zone and the strain-softening zone based on the SMP criterion are both smaller than those based on the Mohr–Coulomb criterion. The radius of the broken zone for the SMP criterion is 4.39 m, which is about 75.82% of that for the Mohr–Coulomb criterion. The radius of the strain-softening zone of the Mohr–Coulomb criterion is 5.70 m, which is about 73.74% of that for the Mohr–Coulomb criterion.

5.1. Effect of the Softening Modulus. In order to analyze the influence of cohesive softening modulus on the deformation of tunnel surrounding rock, the cohesive softening modulus H_c are selected as 200 MPa, 300 MPa, 400 MPa, 500 MPa, and 600 MPa for comparative analysis. The variation of

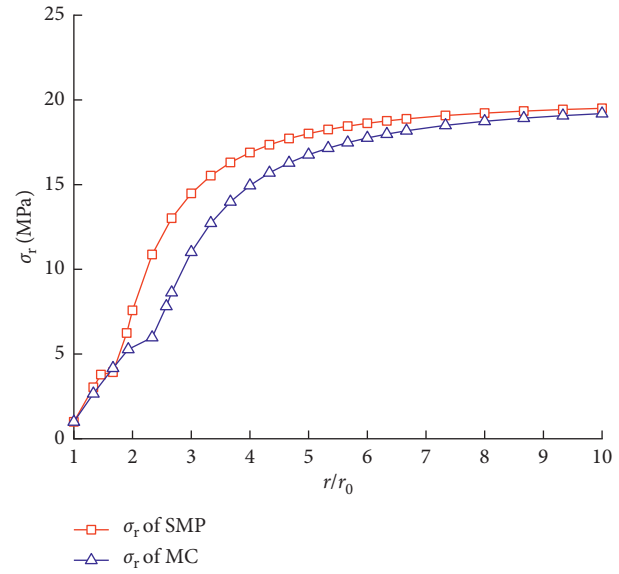

Figure 7: Surrounding rock tangential stress distribution of the Mohr–Coulomb and SMP criteria.

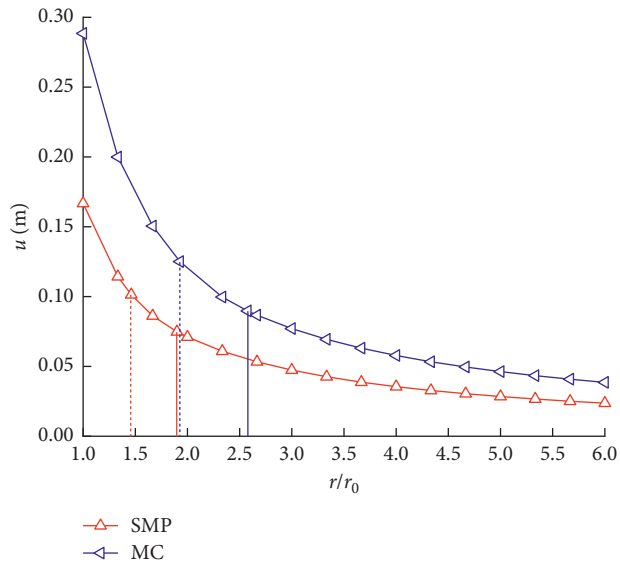

Figure 8: Plastic zone radius and displacement of the Mohr–Coulomb and SMP criteria.

surrounding rock displacement is shown in Figure 9. The dotted vertical line indicates the radius of the broken zone, and the solid vertical line indicates the radius of the strain-softening zone. It can be seen that the cohesive softening modulus H_c has a little effect on the displacement of tunnel surrounding rock. The larger the H_c, the smaller the displacement of the surrounding rock near the tunnel is. H_c has no effect on the radius of the strain-softening zone but has a significant effect on the radius of the broken zone. With H_c increasing, the radius of the broken zone gradually expands, but the extent of expansion becomes smaller and smaller. With H_c increasing, the range of the total plastic zone remains unchanged.

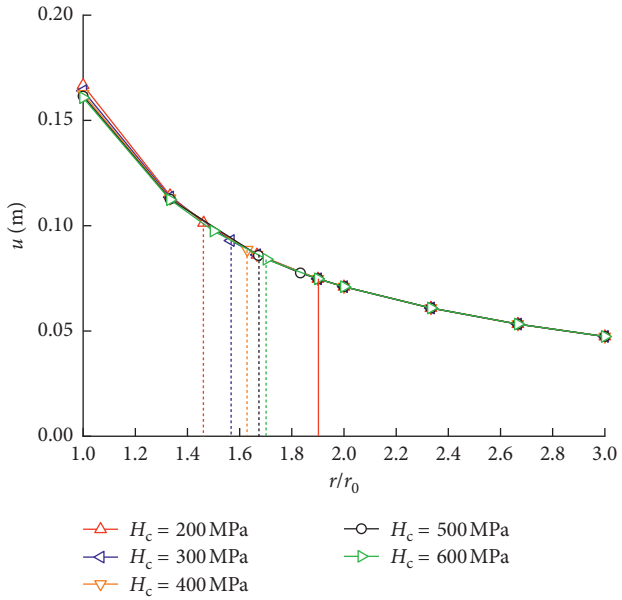

Figure 9: The influence of strain softening on plastic zone radius and displacements.

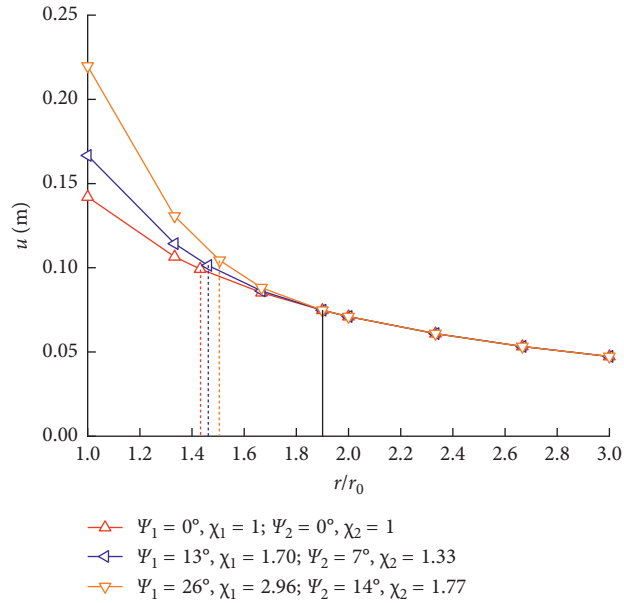

Figure 10: The influence of dilatancy on the plastic zone radius and displacements.

5.2. Effect of the Dilatancy. The dilatancy properties of the tunnel surrounding rock are mainly manifested by the dilatancy angle and the plastic potential function. In this paper, for the associated flow rule ($\psi = \varphi$), nonassociative flow rule ($\psi \neq \varphi$), and irrespective of dilatancy ($\psi = 0$), the corresponding value of the dilatancy coefficient χ is obtained. The softening zone radius, the broken zone radius, and the displacement distribution corresponding to different dilatancy angles are illustrated in Figure 10. It can be seen that the dilatancy angle has a significant influence on the displacement of the plastic zone. The displacement of the tunnel surface for the associated flow rule ($\psi = \varphi$) and for the nonassociative flow rule ($\psi = \varphi/2$) are 21.97 mm and 16.67 mm, respectively. The displacement of the tunnel surface for the dilatancy ($\psi = 0$) is 14.21 mm, which is 85.24% of that for the nonassociative flow rule ($\psi = \varphi/2$). In other words, the associated flow rule takes into account the influence of dilatancy too much, and the actual deformation of the surrounding rock is underestimated without considering the dilatancy. The dilatancy angle has no effect on the radius of the strain-softening zone. However, the larger the dilatancy angle is, the larger the radius of the broken zone is.

5.3. Effect of Internal Friction Angle. To analyze the influence of the internal friction angle on the displacement of surrounding rock, different internal friction angles in the strain-softening zone and the broken zone were selected for analysis. The internal friction angles in the strain-softening zone are selected as 22°, 24°, 26°, 28°, and 30°, respectively. The internal friction angles in the broken zone are selected as 10°, 12°, 14°, 16°, and 18°, respectively. The rock displacement and plastic zone radius are shown in Figure 11. The dotted vertical line indicates the radius of the broken zone, and the solid vertical line indicates the radius of the strain-softening zone.

It can be seen from Figure 11(a) that, as the internal friction angle in the strain-softening zone increases, the displacement of the tunnel surrounding rock decreases. When the internal friction angle in the strain-softening zone is increased from 22° to 30°, the displacement at the tunnel wall is reduced from 19.34 mm to 14.06 mm, which is reduced by 27.30%. As the internal friction angle in the strain-softening zone increases, the radius of the strain-softening zone and the radius of the broken zone decrease. When the internal friction angle in the strain-softening zone is increased from 22° to 30°, the radius of the strain-softening zone is reduced from 6.39 m to 5.08 m, and the radius of the broken zone was reduced from 4.81 m to 3.98 m. It can be seen from Figure 11(b) that, as the internal friction angle increases in the broken zone, the displacement of the tunnel surrounding rock decreases. When the internal friction angle in the broken zone is increased from 10° to 18°, the displacement at the tunnel wall is reduced from 21.85 mm to 13.25 mm, which is reduced by 39.36%. As the internal friction angle in the strain-softening zone increases, the radius of the strain-softening zone and the radius of the broken zone are reduced. When the internal friction angle in the broken zone increases from 10° to 18°, the radius of the strain-softening zone decreases from 6.47 m to 5.11 m and the radius of the broken zone decreases from 4.97 m to 3.96 m.

Therefore, the change of the internal friction angle in the strain-softening zone and the broken zone will affect the displacement distribution of the tunnel surrounding rock. The larger the internal friction angle is, the smaller the displacement of the surrounding rock and the radius of the plastic zone are. The surrounding rock of the broken zone is more sensitive to the internal friction angle than that of the strain-softening zone. In the engineering practice, the deformation of the surrounding rock can be effectively

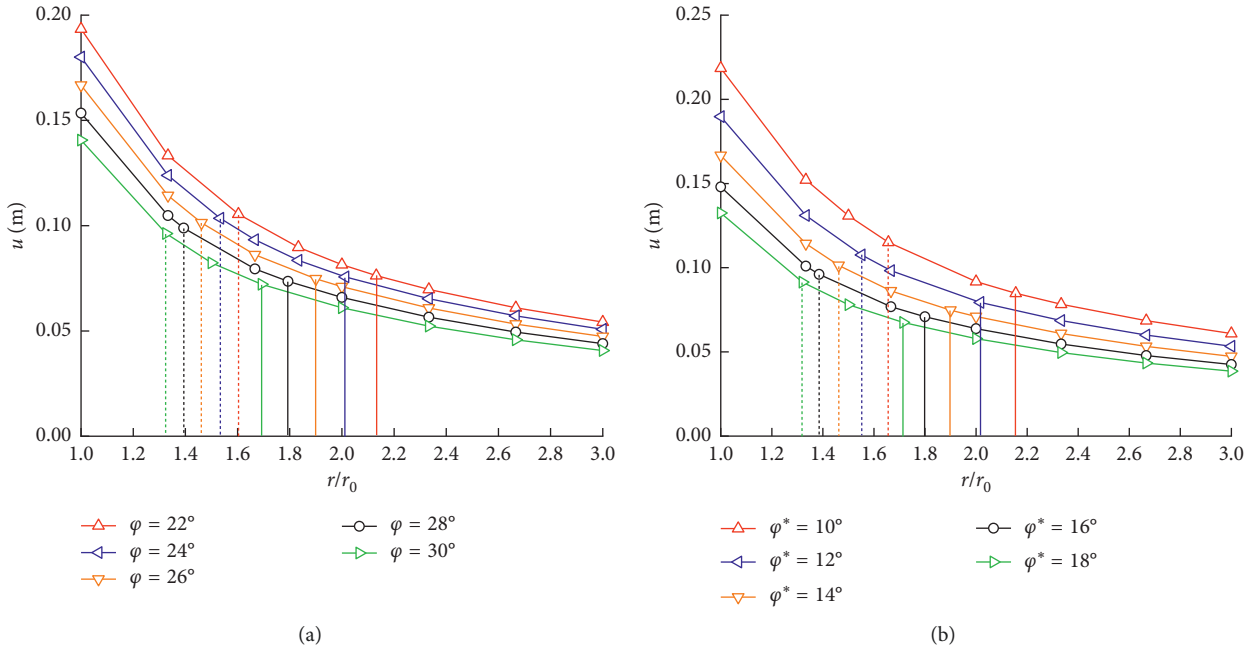

Figure 11: The influence of internal friction angle on plastic zone radius and displacements. (a) Strain-softening zone. (b) Broken zone.

controlled by increasing the internal friction angle in the broken zone of surrounding rock by grouting or other means.

6. Conclusions

According to the strain-softening characteristics of rock mass, an ideal elastic strain-softening model was developed. The circular tunnel surrounding rock is subdivided into plastic broken zone, plastic strain-softening zone, and elastic zone. Based on the generalized SMP criterion, the elastic-plastic analytical solution of the surrounding rock of the circular tunnel was obtained. The effects of intermediate principal stress, strain softening, and dilatancy were considered in the unified solution. The stress distribution, displacement distribution, and plastic zone radius of surrounding rock based on the SMP criterion are compared with those based on the Mohr–Coulomb criterion. The sensitivity of parameters such as softening modulus, dilatancy angle, and internal friction angle were discussed. The results summarized as follows:

(1) The displacement of surrounding rock based on the SMP criterion is generally smaller than that of Mohr–Coulomb criterion. The radius of the broken zone and the strain-softening zone based on the SMP criterion are also smaller than that based on the Mohr–Coulomb criterion.

(2) The softening modulus has a little effect on the displacement of the tunnel surrounding rock but has a significant influence on the radius of the plastic broken zone. With the softening modulus increasing, the range of the broken zone becomes larger, the range of the strain-softening zone decreases, and the range of the total plastic zone remains unchanged.

(3) The dilatancy angle and the internal friction angle have a great significance on the displacement of the tunnel. The deformation of surrounding rock will be underestimated without considering the dilatancy. The larger the internal friction angle is, the smaller the displacement and the radius of the plastic zone are. The surrounding rock in the broken zone is more sensitive to the internal friction angle than the surrounding rock in the strain-softening zone.

Data Availability

The data of this study are available from the corresponding author upon request.

Conflicts of Interest

The authors declare that they have no conflicts of interest.

Acknowledgments

Financial support from the National Natural Science Foundation of China (no. 51774022) and the National Key Research and Development Plan of China (nos. 2017YFC0804101 and 2018YFC0808403) is gratefully acknowledged.

References

[1] S.-Q. Xu and M.-H. Yu, "The effect of the intermediate principal stress on the ground response of circular openings in rock mass," *Rock Mechanics and Rock Engineering*, vol. 39, no. 2, pp. 169–181, 2006.

[2] K. Terzaghi and R. B. Peck, *Soil Mechanics in Engineering Practice*, Wiley, New York, NY, USA, 1948.

[3] S. Wang, X. Yin, H. Tang, and X. Ge, "A new approach for analyzing circular tunnel in strain-softening rock masses,"

International Journal of Rock Mechanics and Mining Sciences, vol. 1, no. 47, pp. 170–178, 2010.

[4] K.-H. Park, B. Tontavanich, and J.-G. Lee, "A simple procedure for ground response curve of circular tunnel in elastic-strain softening rock masses," *Tunnelling and Underground Space Technology*, vol. 23, no. 2, pp. 151–159, 2008.

[5] E. Alonso, L. R. Alejano, F. Varas, G. Fdez-Manin, and C. Carranza-Torres, "Ground response curves for rock masses exhibiting strain-softening behaviour," *International Journal for Numerical and Analytical Methods in Geomechanics*, vol. 27, no. 13, pp. 1153–1185, 2003.

[6] L. R. Alejano, E. Alonso, A. Rodriguez-Dono, and G. Fernandez-Manin, "Application of the convergence-confinement method to tunnels in rock masses exhibiting Hoek–Brown strain-softening behaviour," *International Journal of Rock Mechanics and Mining Sciences*, vol. 1, no. 47, pp. 150–160, 2010.

[7] L. R. Alejano, A. Rodríguez-Dono, and M. Veiga, "Plastic radii and longitudinal deformation profiles of tunnels excavated in strain-softening rock masses," *Tunnelling and Underground Space Technology*, vol. 30, pp. 169–182, 2012.

[8] Q. Zhang, B.-S. Jiang, S.-L. Wang, X.-R. Ge, and H.-Q. Zhang, "Elasto-plastic analysis of a circular opening in strain-softening rock mass," *International Journal of Rock Mechanics and Mining Sciences*, vol. 50, pp. 38–46, 2012.

[9] M. Zhu, Y. Yang, F. Gao, and J. Liu, "Analytical solution of tunnel surrounding rock for stress and displacement based on Lade–Duncan criterion," *Advances in Civil Engineering*, vol. 2018, Article ID 5363658, 7 pages, 2018.

[10] X. Yang, H. Yuan, J. Wu, and S. Li, "Elastoplastic analysis of circular tunnel based on Drucker–Prager criterion," *Advances in Civil Engineering*, vol. 2018, Article ID 5149789, 8 pages, 2018.

[11] M. Singh, A. Raj, and B. Singh, "Modified Mohr-Coulomb criterion for non-linear triaxial and polyaxial strength of intact rocks," *International Journal of Rock Mechanics and Mining Sciences*, vol. 48, no. 4, pp. 546-547, 2011.

[12] H. Jiang and Y. Xie, "A note on the Mohr-Coulomb and Drucker-Prager strength criteria," *Mechanics Research Communications*, vol. 38, no. 4, pp. 309–314, 2011.

[13] L. Bousshine, A. Chaaba, and G. De Saxce, "Softening in stress-strain curve for Drucker-Prager non-associated plasticity," *International Journal of Plasticity*, vol. 17, no. 1, pp. 21–46, 2001.

[14] C. J. Deng, G. J. He, and Y. R. Zheng, "Studies on Drucker-Prager yield criterions based on Mohr-Coulomb yield criterion and application in geotechnical engineering," *Chinese Journal of Geotechnical Engineering*, vol. 28, no. 6, pp. 735–739, 2006, in Chinese.

[15] C. Carranza-Torres, "Elasto-plastic solution of tunnel problems using the generalized form of the Hoek-Brown failure criterion," *International Journal of Rock Mechanics and Mining Sciences*, vol. 41, no. 1, pp. 1–11, 2004.

[16] S. K. Sharan, "Analytical solutions for stresses and displacements around a circular opening in a generalized Hoek-Brown rock," *International Journal of Rock Mechanics and Mining Sciences*, vol. 1, no. 45, pp. 78–85, 2008.

[17] M. Fraldi and F. Guarracino, "Limit analysis of collapse mechanisms in cavities and tunnels according to the Hoek-Brown failure criterion," *International Journal of Rock Mechanics and Mining Sciences*, vol. 46, no. 4, pp. 665–673, 2009.

[18] E. Detournay, "Elastoplastic model of a deep tunnel for a rock with variable dilatancy," *Rock Mechanics and Rock Engineering*, vol. 19, no. 2, pp. 99–108, 1986.

[19] T. Ogawa and K. Y. Lo, "Effects of dilatancy and yield criteria on displacements around tunnels," *Canadian Geotechnical Journal*, vol. 24, no. 1, pp. 100–113, 1987.

[20] L. R. Alejano and E. Alonso, "Considerations of the dilatancy angle in rocks and rock masses," *International Journal of Rock Mechanics and Mining Sciences*, vol. 42, no. 4, pp. 481–507, 2005.

[21] H. Matsuoka and T. Nakai, "Stress-deformation and strength characteristics of soil under three different principal stresses," *Proceedings of the Japan Society of Civil Engineers*, vol. 1974, no. 232, pp. 59–70, 1974.

[22] H. Matsuoka, Y. Yao, and D. Sun, "The Cam-clay models revised by the SMP criterion," *Soils and Foundations*, vol. 39, no. 1, pp. 81–95, 1999.

[23] H. Matsuoka, Y. P. Yao, and M. Ichimura, "A transformed stress based on extended SMP criterion and its application to elastoplastic model for geomaterials," *Doboku Gakkai Ronbunshu*, vol. 2001, no. 680, pp. 211–224, 2001.

[24] Y. P. Yao, D. A. Sun, and H. Matsuoka, "A unified constitutive model for both clay and sand with hardening parameter independent on stress path," *Computers and Geotechnics*, vol. 35, no. 2, pp. 210–222, 2008.

[25] C. Z. Wu, L. D. Yang, and Q. S. Li, "Perfect elastic-brittle-plastic solution of axisymmetric circular openings in rock mass on extended SMP criterion," *Engineering Mechanics*, vol. 8, p. 35, 2013, in Chinese.

[26] Y. L. Lu, L. G. Wang, F. Yang, Y. J. Li, and H. M. Chen, "Post-peak strain softening mechanical properties of weak rock," *Chinese Journal of Rock Mechanics and Engineering*, vol. 29, no. 3, pp. 640–648, 2010, in Chinese.

[27] Y.-K. Lee and S. Pietruszczak, "A new numerical procedure for elasto-plastic analysis of a circular opening excavated in a strain-softening rock mass," *Tunnelling and Underground Space Technology*, vol. 23, no. 5, pp. 588–599, 2008.

[28] J. L. Pan, Z. L. Gao, and F. H. Ren, "Effect of strength criteria on surrounding rock of circular roadway considering strain softening and dilatancy," *Journal of China Coal Society*, vol. 43, no. 12, pp. 3293–3301, 2018, in Chinese.

[29] J.-F. Zou, S.-S. Li, Y. Xu, H.-C. Dan, and L.-H. Zhao, "Theoretical solutions for a circular opening in an elastic-brittle-plastic rock mass incorporating the out-of-plane stress and seepage force," *KSCE Journal of Civil Engineering*, vol. 20, no. 2, pp. 687–701, 2016.